P32 MAPPING OF THE CIRCUMSTELLAR DISK OF α PSA

S.B. Fajardo-Acosta

SIRTF Science Center, California Institute of Technology, Mail Code 220-6, Pasadena, CA 91125, USA

ABSTRACT

This work investigates far-infrared ($60\,\mu$m) mapping techniques of extended emission, in the form of a circumstellar dust disk, of the main-sequence star α PsA. The direct detection of a disk in this system has advanced our understanding of the Vega phenomenon. The analyzed data consist of $60\,\mu$m maps with the PHOT C-100 3×3-pixel far-infrared camera on-board the Infrared Space Observatory (ISO), in the P32 microscanning dedicated mapping mode. The spatial resolution of the maps is ≈ 30 arcsec. A comparison of the map of α PsA with a similar map of the star α Boo, which does not possess circumstellar dust, is presented. The basic technique is to model a point-spread function (PSF) from the latter, and to subtract it from the Vega-type stellar map. The P32Tools algorithm for modelling and correction of transients in P32 maps was applied to both maps in this work. The aim was to check on the reality of previously reported detection of the disk of α PsA in P32 mapping. The P32Tools results confirm α PsA shows extended emission as far as ~ 700 AU from the star. Therefore, the previously reported detections are not an artifact from PHOT detector transients.

Key words: ISO – circumstellar matter – dust, extinction – infrared: stars

1. INTRODUCTION

The direct imaging of circumstellar dust in main-sequence stars is a powerful tool to study possible protoplanetary systems. IRAS observations at $60\,\mu$m spatially resolved circumstellar dust around α Lyr, α PsA, β Pic, and ϵ Eri (review by Backman & Paresce 1993), but these data could not give indications of morphology. Fajardo-Acosta et al. (1997, 1998) imaged the disk of α PsA at $60\,\mu$m with ISO (Kessler et al. 1996). Holland et al. (1998) similarly imaged the disk of α PsA at 850,μm with the James Clerk Maxwell Telescope (JCMT). Other Vega-type systems recently imaged are HR 4796A, measured at 10 and $20\,\mu$m by Koerner et al. (1998) and Jayawardhana et al. (1998), and ϵ Eri, measured with the JCMT at 850 μm (Greaves et al. 1998). More recently, Fajardo-Acosta et al. (2000) reported improved (relative to the results in Fajardo-Acosta et al. 1997, 1998) ISO mapping observations and techniques applied to γ Oph, α PsA, γ Tri, 61 Cyg A, τ^1 Eri, τ Cet, and ϵ Eri. That survey confirmed the detection of extended emission around α PsA.

The resolved dust regions around these sources extend to or beyond $\sim$ 100 AU from the stars. Their thermal emission peaks at far-infrared wavelengths, corresponding to dust temperatures of $\sim$ 50–125 K (Backman & Paresce 1993). These disks are therefore possible analogs in scale to the Solar System's Kuiper Belt (Tremaine 1990).

In order to continue investigations of Kuiper Belt-type disks around main-sequence stars, I investigated the previously reported disk detection around α PsA (Fajardo-Acosta et al. 2000, and references therein). New data analysis tools for ISO mapping observations exist (Section 2.2) that allow to check the reality of extended emission observations, in view of known instrumental artifacts. This work investigates whether such artifacts affected the map of α PsA.

2. OBSERVATIONS AND DATA REDUCTION

2.1. PHOT P32 maps and PIA processing

The $60\,\mu$m map of the Vega-type star α PsA (Table 1) was obtained with the PHOT C-100 3×3-pixel far-infrared array camera (Lemke et al. 1996) on-board ISO. Each pixel subtends 45 arcsec×45 arcsec. It was measured in the PHOT P32 microscanning dedicated mapping mode. The total integration time at each spacecraft raster pointing was 128 seconds. See Fajardo-Acosta et al. 2000.

Maps were reduced with the PHOT Interactive Analysis (PIA) software package [1], version 9.1. The pixels in the reduced maps are 15 arcsec×15 arcsec and the spatial resolution is $\sim$ 30 arcsec. Absolute flux calibration of the maps was done in PIA using Fine Calibration Source 1 (FCS1) measurements.

The reductions presented by Fajardo-Acosta et al. (2000) were done with PIA version

[1] PIA is a joint development by the ESA Astrophysics Division and the ISOPHOT Consortium led by the Max Planck Institute for Astronomy (MPIA), Heidelberg. Contributing ISOPHOT Consortium institutes are DIAS, RAL, AIP, MPIK, and MPIA.

Table 1. List of sources in the ISO mapping study. Columns [2] and [3] list spectral type and Hipparcos distance from the SIMBAD database. Column [4] lists 60 μm flux density (color-corrected assuming a 10^4 K blackbody spectral energy distribution) from the IRAS Faint Source Catalog (Moshir et al. 1992)

Name	Type	D (pc)	IRAS $F_\nu (60\,\mu\mathrm{m})$ (Jy)
α PsA	A3 V	7.69	7.34±0.57
α Boo PSF	K1.5 III	...	19.5±2.9

7.3.2, and the program IMAP[2] was run to improve flat-fielding, vignetting, and long-term drift corrections. IMAP was not applied in the present work.

2.2. P32Tools processing of maps

After standard processing with PIA, I run the P32Tools program[3] to model, and correct for, transients in the C100 detector and their effects on P32 maps. P32Tools aims at correcting effects from illumination steps, particularly under low illumination. The main effects of such steps are signal undershoot (on short timescales), hook response, slow convergence to asymptotic response, and signal glitches. The following particular procedure was applied to the maps in this work, within P32Tools and PIA: Signal was conditioned with the standard ERD2MAP routine. Test trials on manual deglitching and patching of gaps did not yield any improvement since the observed stars are fairly bright. Therefore deglitching and patching were not applied. Following ERD2MAP, drift-fitting parameters were calculated in a standard procedure. Attempts at self calibration (manual fine-tunning of transient model parameters) did not yield improvements. At the end of P32Tools processing, and back into PIA (SCP stage), manual discarding of signals, clearly below a baseline, yielded corrections for undershoot, This correction was applied individually for each pixel.

The star α Boo (Table 1) is known not to have any dust around it. α Boo was measured to model the response of PHOT to a true point source, as described in the following section.

[2] IMAP was developed by N. Lu and M. Hur at the Infrared Processing and Analysis Center (IPAC), Jet Propulsion Laboratory, California Institute of Technology.

[3] The algorithm for P32Tools was developed by R. Tuffs (MPIK), and its integration to PIA and software interface were developed at the ISO Data Centre (IDC ESA), and IPAC.

Section 4.1 compares the results of using either IMAP, or P32Tools, and the two versions of PIA, in detection of extended emission in α PsA relative to α Boo.

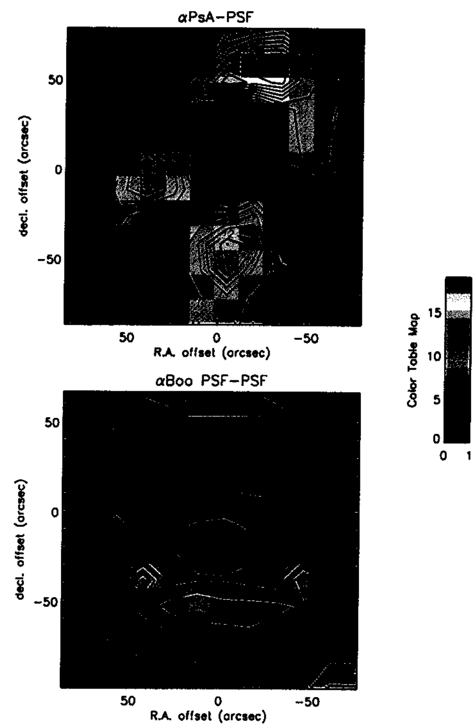

Figure 1. Grayscale and contour plots of PHOT P32 maps of stellar sources, after subtraction of a model PSF fitted from the map of α Boo. The mean background level was also subtracted, and surface brightness is in units of the background noise (σ). The top panel is the map of α PsA. The bottom panel is the map of α Boo's residuals. The red cross marks the position of the star (before PSF subtraction). The red arrow is the raster scan direction during each P32 observation. North is up and east to the left. Contour levels are: 0, 6, 12, 16, 20 σ (top panel), and 2, 4, 6, and 8 σ (bottom panel).

3. EXTENDED EMISSION IN P32 MAPS

The Image Reduction and Analysis Facility (IRAF) software package (Tody 1986), version 2.11, was used to analyze the maps. A two-dimensional point-spread function (PSF) model was fitted to the map of α Boo, as described in Fajardo-Acosta et al. (2000). The model PSF was subtracted from the stellar image in the α PsA map. The background noise (standard deviation) is the dominant term in the uncertainty in surface brightness in the maps.

Two criteria were then employed to search for extended emission in the PSF-subtracted Vega-type map:

First, I evaluated the peak surface brightness above the background, in units of the background uncertainty. If this peak was larger than in the PSF subtracted map of α Boo, then extended emission was deemed possible. Fig-

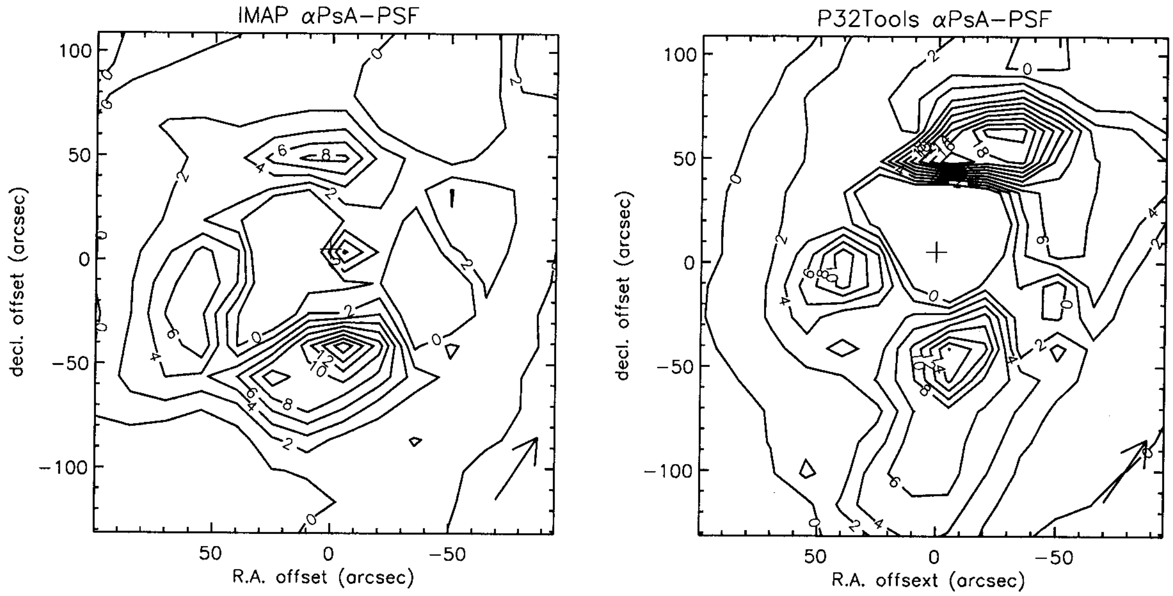

Figure 2. Contour plots of P32 maps of α PsA, after background and PSF (α Boo) subtraction. Surface brightness levels are expressed as in Figure 1. Left panel: map reduced with PIA 7.3.2 and IMAP processing (Fajardo-Acosta et al. 2000). Right panel: map reduced with PIA 9.1 and P32Tools. The red crosses and arrows are as explained in Figure 1. Contour levels start at 2 σ, in steps of 2 σ, and up to 18 σ (left panel), and 20 σ (right panel).

ure 1 shows grayscale and contour plots of PSF-subtracted (and median background-subtracted) maps of α PsA (top panel) and the PSF reference star α Boo (bottom panel). Figure 1 illustrates that the peak in α PsA's map ($\sim 21\ \sigma$) is significantly larger than in the PSF reference α Boo ($\sim 6\ \sigma$). Therefore, Figure 1 shows that the P32 map of α PsA has extended emission, relative to the PSF from α Boo.

Second, I summed the surface brightness of PSF-subtracted maps, over a 60 arcsec-radius circular area centered at the star's position. I defined such area as the "vicinity" of the star; it encloses practically all of the PSF that was subtracted. I also evaluated the standard deviation of the above sum, and denoted it by σ(Bright.). If the relative σ(Bright.) of a star is smaller than that of the PSF reference star, then it is possible that there is extended emission in the vicinity of such star. The relative σ(Bright.) of α Boo was 188 per cent, whereas that of α PsA was much smaller, 26 per cent. Therefore, there is significant extended emission around the latter.

4. DISCUSSION

4.1. Comparison of P32Tools and IMAP results

The PSF-subtracted map of α PsA in Fajardo-Acosta et al. (2000), using also α Boo as a reference PSF, exhibited very similar (relative to Section 3) properties in regards to the search for extended emission. The peak surface brightness above the background was $\sim 18\ \sigma$, vs. $\sim 6\ \sigma$ for α Boo. The relative σ(Bright.) in α PsA was 13 per cent, vs. 72 per cent for α Boo.

Therefore, the use of P32Tools and the earlier use of IMAP yield a consistent detection of extended emission around α PsA. Instrumental artifacts such as transients during P32 mapping are therefore not spuriously creating the features we see in the vicinity of the Vega-type star.

Figure 2 shows a comparison of the PSF-subtracted maps of α PsA reduced with PIA 7.3.2 and IMAP, by Fajardo-Acosta et al. (2000) (left panel) and PIA 9.1 and P32Tools (right panel). The latter is the same as Figure 1, top panel. We see from Figure 2 that both reductions yield peak extended emission to the north and south of the star, at comparable levels above the background. The morphologies of both maps of α PsA are roughly similar. The difference between the north and south peak levels are not significant, since within each map they differ by $\sim 6\ \sigma$, which is the size of the residuals in the PSF reference star (Figure 1, bottom panel).

4.2. Extended emission around α PsA

The extended emission detected around α PsA (Figure 2, right panel, and Figure 1, top panel) is seen at levels $> 2\ \sigma$ above the background, at distances 30–100 arcsec, or $\sim$ 200–700 AU from the star. The extended emission features suggest there is a nearly edge-on disk of dust around the star, aligned in the north-south direction. This conclusion confirms the findings from JCMT 850 μm (sub-mm) observations (Holland et al. 1998). The range of distances of 60 μm emission agrees with the range $\sim$ 210–560 AU inferred by Fajardo-Acosta et al. (1997, 1998). Together with the IRAS 25, 60, and 100 μm color temperatures of α PsA, of $\sim$ 58–75 K, the range of locations of dust implies grain sizes of 4–10 μm around α PsA (Fajardo-Acosta et al. 1997, 1998). On the other hand, the 850 μm map of α PsA measured by Holland et al. (1998) shows dust closer to the star, at distances 30–315 AU, peaking at $\sim$ 80 AU. The grains seen in the sub-mm images would have sizes > 60 μm, in order to explain the IRAS color temperatures and the above locations. The grains seen in the sub-mm images are confined to annuli that resemble the Kuiper Belt of our Solar System (Holland et al. 1998). To explain why one sees in the ISO maps smaller grains (4–10 μm) further out from α PsA than in the sub-mm image, it could be that these small grains are released at periapses in the Kuiper Belt-type regions from parent cometary bodies. Radiation pressure would displace the smallest of these grains to new, bound orbits more eccentric than those of their parent comets. These new orbits would extend beyond the "Kuiper Belts," and the grains would spend more time at their apoapses, where one might be detecting them in the ISO images.

ACKNOWLEDGEMENTS

This work was carried out at the SIRTF Science Center, California Institute of Technology, under contract with NASA. It is based on observations with ISO, an ESA project with instruments funded by ESA Member States (especially the PI countries: France, Germany, the Netherlands and the United Kingdom) and with the participation of ISAS and NASA. The research has made use of the SIMBAD database, operated at CDS, Strasbourg, France.

REFERENCES

Backman, D.E., Paresce, F., 1993, Main-Sequence Stars With Circumstellar Solid Material: The Vega Phenomenon. In: Levy, E.H., Lunine, J.I., Mathews, M.S. (eds.) Protostars and Planets III. Univ. Arizona Press, Tucson. p. 1253

Fajardo-Acosta, S.B., Stencel, R.E., Backman, D.E., 1997, ApJ 487, L151

Fajardo-Acosta, S.B., Stencel, R.E., Backman, D.E., 1998, ApJ 503, L193

Fajardo-Acosta, S.B., Backman, D.E., Stencel, R.E., 2000, ISOPHOT Mapping of Vega-type Circumstellar Dust. In: Laureijs, R.J., Leech, K., Kessler, M.F. (eds.) ISO Beyond Point Sources: Studies of Extended Infrared Emission. ESA SP-455. ESA-ESTEC, Noordwijk. p. 73

Greaves, J.S., Holland, W.S., Moriarty-Schieven, G., et al., 1998, ApJ 506, L133

Holland, W.S., Greaves, J.S., Zuckerman, B., et al., 1998, Nature 392, 788

Jayawardhana, R., Fisher, S., Hartmann, L., et al., 1998, ApJ 503, L79

Kessler, M. F., Steinz, J.A., Anderegg, M.E., et al., 1996, A&A 315, L27

Koerner, D.W., Ressler, M.E., Werner, M.W., Backman, D.E., 1998, ApJ 503, L83

Lemke, D., Klaas, U., Abolins, J., et al., 1996, A&A 315, L64

Moshir, M., et al., 1992, Explanatory Supplement to the IRAS Faint Source Survey, Version 2, JPL D-10015 8/92. JPL, Pasadena

Tody, D., 1986, Proc. SPIE 627, 733

Tremaine, S., 1990, Dark Matter in the Solar System. In: Lynden-Bell, D., Gilmore, G. (eds.) Baryonic Dark Matter. Kluwer, Dordrecht. p. 37